JACS
JOURNAL OF THE AMERICAN CHEMICAL SOCIETY

pubs.acs.org/JACS

Article

Influence of Dielectric Environment upon Isotope Effects on Glycoside Heterolysis: Computational Evaluation and Atomic Hessian Analysis

Katarzyna Świderek, Alexander J. Porter, Catherine M. Upfold, and Ian H. Williams*

Cite This: J. Am. Chem. Soc. 2020, 142, 1556−1563

Read Online

ACCESS | Metrics & More | Article Recommendations | Supporting Information

ABSTRACT: Isotope effects depend upon the polarity of the bulk medium in which a chemical process occurs. Implicit solvent calculations with molecule-shaped cavities show that the equilibrium isotope effect (EIE) for heterolysis of the glycosidic bonds in 5′-methylthioadenosine and in 2-(*p*-nitrophenoxy)tetrahydropyran, both in water, are very sensitive in the range $2 \leq \varepsilon \leq 10$ to the relative permittivity of the continuum surrounding the oxacarbenium ion. However, different implementations of nominally the same PCM method can lead to opposite trends being predicted for the same molecule. Computational modeling of the influence of the inhomogeneous effective dielectric surrounding a substrate within the protein environment of an enzymic reaction requires an explicit treatment. The EIE (K_H/K_D) for transfer of cyclopentyl, cyclohexyl, tetrahydrofuranyl and tetrahydropyranyl cations from water to cyclohexane is predicted by B3LYP/6-31+G(d) calculations with implicit solvation and confirmed by B3LYP/6-31+G(d)/OPLS-AA calculations with averaging over many explicit solvation configurations. Atomic Hessian analysis, whereby the full Hessian is reduced to the elements belonging to a single atom at the site of isotopic substitution, reveals a remarkable result for both implicit and explicit solvation: the influence of the solvent environment on these EIEs is essentially captured completely by only a 3 × 3 block of the Hessian, although these values must correctly reflect the influence of the whole environment. QM/MM simulation with ensemble averaging has an important role to play in assisting the meaningful interpretation of observed isotope effects for chemical reactions both in solution and catalyzed by enzymes.

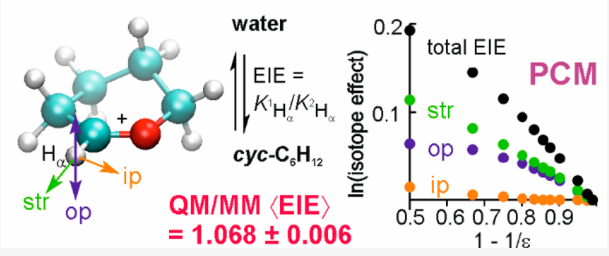

INTRODUCTION

Kinetic isotope effects (KIEs) are a powerful experimental tool for transition-state (TS) analysis of mechanisms of reactions in chemistry and biochemistry,[1,2] provided that their values may be meaningfully interpreted. It is often assumed that trends in KIEs may be related to structural changes in TSs understood in terms of geometries and bond orders,[3,4] but recent computational studies have suggested that changes in the electrostatic environment of a TS may also be significant.[5−7] The deuterium (^2H = D) equilibrium isotope effect (EIE) for transfer of CH_3^+ from a vacuum to a dielectric continuum varies very significantly for $2 \leq \varepsilon \leq 10$,[5] usually considered as the range of values of the static relative permittivity ε in an enzyme active site.[8] It is conceivable that a reaction involving charge redistribution, separation, or neutralization within an enzyme active site could manifest variations in KIEs, as between wild-type and mutant enzymes, that originate from changes in the effective dielectric within the inhomogeneous protein environment; if so, there would be important implications for the interpretation of experimental KIEs in mechanistic enzymology.

Although solvent effects on reaction mechanisms are well-known,[9] solvent effects *on* isotope effects are less well understood. Changing the solvent can alter a KIE *indirectly* by affecting the TS structure.[10] For example, a more polar solvent may stabilize the ionic product in Menshutkin reaction more effectively and give an "earlier" TS, as accounted for by the Hammond postulate, which in turn may give rise to a less inverse secondary (2°) α-D KIE.[11,12] The rate-determining step in solvolyses of 2-propyl substrates shifts from substitution to ionization and then to dissociation within an S_N2-S_N1 mechanistic spectrum, as the solvent becomes more ionizing and less nucleophilic.[13] Changing the solvent can also alter a KIE indirectly by affecting the mechanism: in Shiner's generalized model for solvolytic substitution at saturated carbon, changing the solvent may alter the identity of the rate-determining step as indicated by the magnitude and direction of the measured 2° α-D KIE.[14] Bentley has questioned several assumptions within Shiner's model, including that single-step α-D KIEs for non-S_N2 mechanisms are independent of solvent,

Received: November 6, 2019
Published: December 30, 2019

https://dx.doi.org/10.1021/jacs.9b11988
J. Am. Chem. Soc. 2020, 142, 1556−1563

and has suggested that solvolyses of secondary alkyl sulfonates can be rationalized by a model combining heterolysis with nucleophilic solvent participation.[15] The very small influence of solvent on 2° α-D and β-D_3 KIEs for solvolysis of (1-chloroethyl)benzene in aqueous ethanol of varying proportions might indicate subtle mechanistic change,[16] but it may be noted that the solvent mixtures considered were all polar ($35 < \varepsilon < 55$). KIEs may be influenced by solvation that affects isotopically sensitive vibrational frequencies *directly*, regardless of TS structure or the identity of a rate-determining step. This has recognized in largely overlooked work by Keller and Yankwich, who investigated simple models that might allow medium effects on heavy-atom KIEs to be estimated.[17−19]

The matrix of second derivatives of energy with respect to Cartesian coordinates (the Hessian) plays a key role in the theory of molecular vibrations and of isotope effects, since its mass-weighting and diagonalization leads to the normal modes and associated harmonic frequencies; the same Hessian is used for each isotopolog with different masses as appropriate. The traditional ("molecular") approach to EIE or KIE calculations considers the Hessian for a whole molecule at a stationary point on a potential-energy surface, but the use of QM/MM methods for large condensed ("supramolecular") systems involves use of a Hessian for only a subset of atoms which are not in themselves at a stationary point.[20] This raises a question: what size does the subset need to be in order for its Hessian to yield reliable values for isotope effects?

We now report on EIEs computed for heterolysis of a glycoside in water leading to formation of an oxacarbenium cation in a nonpolar medium, and for transfer of some carbenium and oxacarbenium ions from water to cyclohexane. Variations in these IEs are successfully analyzed in terms of the influence of the dielectric environment upon the "atomic Hessian" at the single site of isotopic substitution by means of both implicit and explicit solvent treatments.

COMPUTATIONAL METHODS

Continuum Solvation. Geometry optimization and frequency calculations for 5′-methylthioadenosine (MTA) and 5′-methylthioribosyl cation (MTR) were performed with Gaussian 09[21] using the B3LYP density functional with the aug-cc-pVDZ basis; this functional was employed for consistency with previous work,[5,6,22,23] since it has been identified as leading to reliable estimates of harmonic vibrational frequencies.[24] Continuum solvation by the Onsager method with a spherical cavity used solute radii obtained from a gas-phase molecular volume calculation. Continuum solvation by the Polarized Continuum Model (PCM) used UFF atomic radii to specify a molecule-shaped cavity. Geometry optimization and frequency calculations for cyclopentyl (CP), tetrahydrofuranyl (THF), cyclohexyl (CH), and tetrahydropyranyl (THP) cations were performed with Gaussian 16[25] (G16) using B3LYP with either the 6-31+G(d) or the aug-cc-pVDZ basis. The DFT integration grid size was explicitly specified. The G09defaults keyword was used to run Gaussian16 jobs using Gaussian09 (G09) default settings.

Isotopic Partition Function Ratios (IPFRs) and EIEs. Mass-weighting and diagonalization of the computed Hessian yielded $3N$ nonzero harmonic vibrational frequencies (for an N-atomic molecule). These frequencies, together with the atomic masses and Cartesian coordinates, were used within the standard harmonic-oscillator, rigid-rotor, ideal-gas approximations to obtain molecular partition functions q as products of translational, rotational, and vibrational (including zero-point energy) factors, from which IPFRs ($f = q_{heavy}/q_{light}$) were obtained by means of the LIPFR program from the SULISO suite of utilities.[26] Spurious translational and rotational contributions to the computed Hessian were projected out (by means of the CAMVIB program from the SULISO suite) to yield six zero frequencies and $3N - 6$ nonzero frequencies corresponding to pure vibrational modes.[27,28] The tritium ($^3H = T$) EIE $(K_H/K_{\alpha-T})_\varepsilon$ for heterolysis of MTA in "water" leading to MTR cation in a continuum with relative permittivity ε was obtained as the ratio $(f_{MTA})_{78}/(f_{MTR})_\varepsilon$.

Atomic Hessian Analysis. The Hessian matrices of Cartesian force constants for the THP and MTR cations have dimensions of 45 × 45 and 57 × 57, respectively. Deletion of all rows and columns, except for those belonging to the H_α atom at the site of isotopic substitution, gave a 3 × 3 matrix in each case which, when mass-weighted and diagonalized in the usual way, yielded three nonzero eigenvalues and three corresponding eigenvectors. Inspection of these normal modes enabled their assignment as "stretching" along the C_α−H_α axis and "bending" in and out of the plane of the carbenium center at C_α.

Basis Set Dependence of EIEs. Figure S1 (Supporting Information) shows that the magnitude of the α−T EIE for heterolysis of MTA (in a continuum with $\varepsilon = 78$) to MTR cation (in a continuum with $2 \le \varepsilon \le 80$) is consistently slightly larger (more normal) for all values of ε. The corresponding α−T EIEs for transfer of MTR cation from $\varepsilon = 80$ to less-polar media are almost identical, with only a very small difference at $\varepsilon = 2$. Accordingly, although the initial study of MTA heterolysis employed the larger aug-cc-pVDZ basis, all further computations in this study were performed with the smaller 6-31+G(d) basis.

QM/MM Calculations. Initial coordinates for the cations and cyclohexane were obtained from gas-phase geometry optimizations, and a pre-equilibrated cubic box of side length of 31.40 Å containing 1034 TIP3P water molecules was used. A cubic box of side length of 45.13 Å containing 512 cyclohexane molecules was constructed by means of the Packmol program,[29] and fDynamo[30,31] was used with OPLS-AA parameters (standard atom types for saturated C and H) to perform initial L-BFGS-B energy minimization (1000 steps) followed by 100 ps of molecular dynamics (MD) at 298 K. All MD simulations employed the Langevin−Verlet algorithm with a 1 fs time step within the NVT ensemble and periodic boundary conditions. B3LYP/6-31+G(d) optimized coordinates for each cation were inserted into the center of each solvent box, and all solvent molecules possessing a non-hydrogen atom within a specified distance of any non-hydrogen atom of the cation were deleted. Energy minimization (1000 steps, as above) of flexible solvent around frozen cation solute was followed by 100 ps MD simulation (as above) with the QM/MM potential. For the purpose of obtaining a representative sample of solvent configurations, it was computationally efficient to describe the frozen cation (with its DFT-optimized geometry) by means of the semiempirical AM1 method in the MD simulation, with MM parameters for water (TIP3P) or cyclohexane (OPLS-AA). A sequence of 48 "snapshot" structures was extracted at 1 ps intervals from the second half of each MD trajectory. Subsequently, for each snapshot, the MM solvent molecules were frozen and a B3LYP/6-31+G(d) relaxation of the cation was performed using a combination of fDynamo with G16. Within each macroiteration of the optimization algorithm, a single-point G16 gradient evaluation was performed within the field of the point-charges of the MM atoms, and the resulting ESP charges and gradients for the QM atoms were passed back to fDynamo for subsequent microiterations for energy minimization of the whole flexible solute (including its six external degrees of freedom) within the frozen solvent environment. The vibrational Hessian was determined for each suitably converged QM structure within its frozen MM environment, resulting in $3N$ nonzero vibrational frequencies for an N-atomic solute. These frequencies, together with the atomic masses and Cartesian coordinates, were used within the harmonic-oscillator approximation to obtain molecular partition functions q as products of vibrational (including zero-point energy) factors, from which IPFRs (f) were obtained by means of eq 1 as implemented in the UJISO program from the SULISO suite of utilities.

https://dx.doi.org/10.1021/jacs.9b11988
J. Am. Chem. Soc. 2020, 142, 1556−1563

$$f_{\text{cation}} = q_{\text{heavy}}/q_{\text{light}} = \prod_{i}^{3N} \sinh\left(\frac{1}{2}u_i\right)_{\text{H}} / \sinh\left(\frac{1}{2}u_i\right)_{\text{D}} \quad (1)$$

Here N is the number of QM atoms, $u_i = hc\omega_i/k_BT$, ω_i is an unscaled harmonic frequency (as a wavenumber/cm^{-1}), T is the absolute temperature, h is Planck's constant, c is the velocity of light, and k_B is Boltzmann's constant. The EIE for transfer of each cation from water to cyclohexane was obtained by means of eq 2 (cf. ref 32).

$$\langle K_H/K_D\rangle = \langle f_{\text{cation}}\rangle_{\text{water}}/\langle f_{\text{cation}}\rangle_{\text{cyclohexane}} \quad (2)$$

RESULTS AND DISCUSSION

Implicit Solvation: Influence of Cavity Shape and Hessian Contamination on EIEs for Heterolysis. It was reported that DFT calculations of the α-T EIE for heterolysis (Scheme 1) of the N-glycosidic bond in MTA were virtually insensitive to variation in the value of ε employed in a continuum solvation model for the MTR cation.[33] Our B3LYP/aug-cc-pVDZ calculations using the Onsager solvation method with a spherical cavity also show essentially no change in this EIE over the range $2 \le \varepsilon \le 80$ (Figure 1). However, use of PCM with a molecule-shaped cavity reveals significant variation of the EIE over the same range of ε: a less-polar medium gives a looser α-CH bond, leading to a more normal EIE for carbenium ion formation. The sensitivity of the EIE to relative permittivity is captured only by use of an appropriately shaped cavity. The clear trend in the results implies that interpretation of the experimental KIE for hydrolysis of MTA catalyzed by MTA nucleosidase (intrinsic $k_H/k_{\alpha T}$ = 1.235),[33] should include consideration of the electrostatic environment of the TS and intermediate as well as the geometrical changes that accompany bond breaking and rehybridization at the anomeric center.

Scheme 1. Heterolysis Equilibrium for MTA Showing Isotopic Substitution

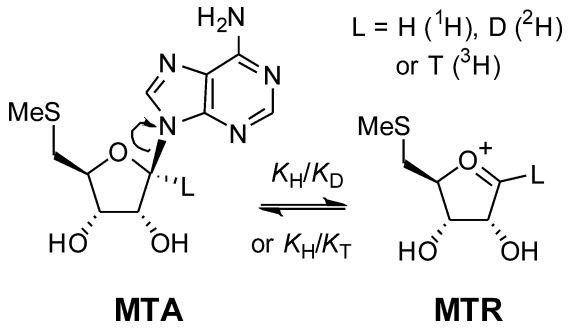

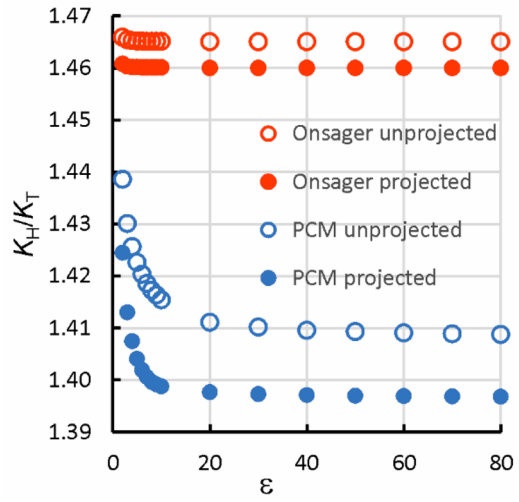

Figure 1. B3LYP/aug-cc-pVDZ α–T EIEs for heterolysis of MTA (ε = 78) to MTR ($2 \le \varepsilon \le 80$) at 298 K using continuum solvation models: Onsager with spherical cavity (red) and PCM with UFF cavity (blue), with (solid) and without (open) projection to remove spurious translational and rotational contributions.

According to the Teller–Redlich product rule,[34,35] there should be equality between the "mass and moment-of-inertia" (MI) term and the "vibrational product" (VP) term for a pair of isotopologous species; the former depends only on the atomic masses and Cartesian coordinates, and the latter only on the harmonic frequencies. If $3N$ frequencies were to be employed, then there would be double counting of the six degrees of freedom corresponding to overall translation and rotation of the molecule. If, however, the six lowest frequencies are omitted from the evaluations of the vibrational partition functions and of the vibrational product terms, then there is inequality between the MI and VP terms; typically, this is in the second decimal place and corresponds to a difference of up to about 1%. Projecting out the spurious translational and rotational contributions from the computed Hessian yielded six zero frequencies and $3N - 6$ nonzero frequencies corresponding to pure vibrational modes; using these frequencies gave MI and VP that differed only in about the sixth decimal place and corresponding to a difference of about 10^{-4} %. Figure 1 also illustrates the effect of this projection: a small but significant difference in the isotope effect. It is not recommended to employ vibrational frequencies obtained directly from unprojected Hessians in isotope-effect calculations.

Hydrolysis of 2-(p-nitrophenoxy)tetrahydropyran in water proceeds by the S_N1 mechanism via the intermediate THP cation (Scheme 2). The calculated B3LYP/aug-cc-pVDZ/

Scheme 2. Heterolysis Equilibrium for MTA Showing Isotopic Substitution

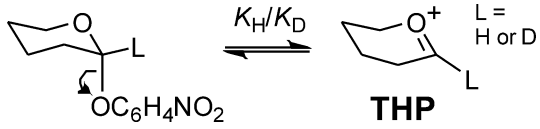

PCM EIE (α-D, 298 K) for this heterolysis in water is 1.235. The corresponding KIE ($k_H/k_{\alpha D}$ = 1.19) for this reaction was measured by Maskill and co-workers in order to shed mechanistic light on enzyme-catalyzed glycoside hydrolysis.[36] It is of interest to consider how the EIE for heterolysis of the acetal in water (a simple model for a glycoside) depends on the relative permittivity of the dielectric continuum surrounding the THP cation, mimicking an oxacarbenium intermediate in the active site of a glycosidase. Our calculations have shown that the EIE varies significantly, particularly for $2 \le \varepsilon \le 10$, giving K_H/K_D = 1.258 at ε = 2.[23] Since the IPFR for the neutral acetal varies only slightly with ε, the EIE for the heterolysis occurring wholly (and hypothetically) within a very nonpolar medium is predicted to be very similar to the value given above, viz. 1.251 at ε = 2. The reaction was studied experimentally in 50% aqueous trifluoroethanol and in 50% aqueous ethanol,[36] but as these are both polar media, any

https://dx.doi.org/10.1021/jacs.9b11988
J. Am. Chem. Soc. 2020, 142, 1556–1563

variation in the KIE might be more indicative of nucleophilic solvent participation than of any influence of a dielectric effect that might be manifest only in very nonpolar media.

Atomic Hessian Analysis. The B3LYP/aug-cc-pVDZ/PCM EIEs (α-D, 298 K) for transfer of both THP and MTR from "water" (ε = 78) to a less polar continuum ($2 \leq \varepsilon \leq 80$) have been computed using both the full Hessian matrices (45 × 45 and 57 × 57, respectively) and "atomic" Hessians (each 3 × 3) for the site of isotopic substitution alone, obtained by removing all elements except those associated with the single atom, with unchanged values. Remarkably, there are near-perfect linear correlations (Figure 2a and 2b) between the EIEs

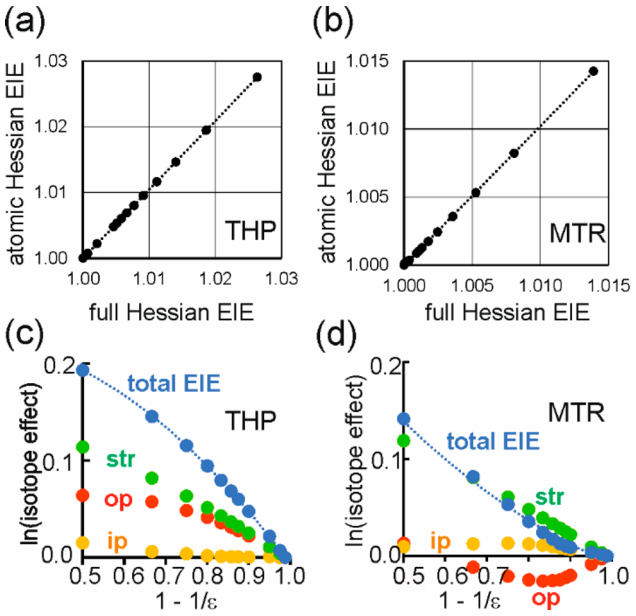

Figure 2. Correlation of full- and atomic-Hessian B3LYP/aug-cc-pVDZ/PCM α-D EIEs (298 K) for transfer of (a) THP and (b) MTR from ε = 78 to a dielectric continuum ($2 \leq \varepsilon \leq 80$). Analysis of stretching (str), in-plane (ip), and out-of-plane (op) components of atomic-Hessian EIEs, expressed as natural logarithms, for (c) THP and (d) MTR as a function of relative permittivity.

resulting from the full and atomic Hessians over the range of ε: linear regression ($EIE_{atomic} = mEIE_{full} + c$) yields m = 1.044, c = −0.044 for THP and m = 1.025, c = −0.025 for MTR, with the goodness of fit (r^2) differing from unity in only the sixth or fourth decimal place, respectively. In summary: all the variation is captured by the influence of the dielectric upon the isotopically substituted atom alone.

This method of atomic Hessian analysis, in which a larger Hessian is pared back to a very small one, is not the same as a traditional "cutoff" procedure[37,38] in which an isotope-effect calculation is performed for a model system containing only atoms within a certain number bonds (typically 2) from the site of isotopic substitution.[39] It must be emphasized that the remaining elements of the pared Hessian are evaluated with the environment of the full system, whereas the included elements of the cutoff Hessian are evaluated in the absence of any environmental influences. However, it can easily be verified that an atomic Hessian determined by (say) numerical differentiation of analytical gradients for a single atom within the environment of a much larger system is identical to one obtained by paring back the full-size Hessian computed with the same system.

The eigenvalues and eigenvectors of the mass-weighted atomic Hessian yield vibrational frequencies and modes for motion of the hydrogen atom at the site of isotopic substitution. Despite the absence of the rest of the molecule, there is a clearly assignable "CH" stretching mode (str) for THP cation with frequencies in the range 3045 cm^{-1} (ε = 80, "water") to 3028 cm^{-1} (ε = 2, "cyclohexane"). Similarly, there is an in-plane bending (ip) mode with frequencies in a narrow range from 1328 to 1326 cm^{-1}, and an out-of-plane (op) bending mode whose frequency varies between 859 cm^{-1} (water) to 848 cm^{-1} (cyclohexane). Insertion of each of these ^{1}H-atom frequencies, along with their ^{2}H-atom counterparts, into the harmonic-oscillator expression for the vibrational partition function yields three factors contributing to the total atomic-Hessian EIE. It is useful to plot their natural logarithms as additive components (Figure 2c for THP and Figure 2d for MTR) against $1 - 1/\varepsilon$ (which is proportional to the electrostatic free energy of solvation in the Born model for a point charge in a spherical cavity)[40] as this represents a novel type of free-energy relationship. In the case of THP, each term is approximately linear: both the "str" and "op" modes contribute to the overall IE, with a negligible contribution from "ip". The IE is consistently normal (>1): the lighter isotopolog prefers a medium with lower polarity. In the case of MTR, the stretching term ln(str) is also linear, reflecting the very good linear correlation that exists between the CH frequencies themselves and $1 - 1/\varepsilon$. However, variation in the ln(ip) and ln(op) terms is distinctly nonlinear and in opposite directions, which approximately cancel each other. Although the variation of the overall EIE with ε is completely reproduced by the influence of the continuum on the Hessian at the site of isotopic substitution alone, it seems that the vibrational frequencies and their isotopic shifts for the bending modes of this atom (i.e., motions transverse to the direction of its covalent attachment to the rest of the molecule) depend on specific characteristics of the UFF cavity shape with the PCM implementation that are not understood. In particular, the contrasting behavior of the frequency for the "op" mode in THP and MTR cations with changing ε is to be noted.

An alternative to using the function $1 - 1/\varepsilon$ for the abscissa, in plots of the dependence of EIEs (or their natural logarithms) on the relative permittivity of the medium, is to employ the function $2(\varepsilon - 1)/(2\varepsilon + 1)$ that appears in Onsager's equation for the electrostatic contribution to the free energy of solvation.[41] However, since the form of the resulting plots does not differ substantially from those shown in Figures 2c and 2d (and others), we prefer to use the simpler function.

Implicit Solvation: Influence of DFT Integration Grid on EIEs for Phase Transfer. Figure 3a shows B3LYP/6-31+G(d) PCM/UFF α−T EIEs (298 K) for transfer of MTR cation from ε = 80 to a dielectric continuum ($2 \leq \varepsilon \leq 80$), as a function of relative permittivity, for a range of popular DFT integration grids sizes. It has recently been pointed out that use of grids that are too small can lead to significant errors in computed vibrational frequencies and derived free energies.[42] Using G09 defaults with the PCM method in G16 indicates a monotonic trend of increasingly normal (>1) EIEs as ε decreases for every grid size considered. (Note that only a small number of values of ε needs to be considered in order to span the range of electrostatic free energies delineated by the function $1 - 1/\varepsilon$ evenly and adequately.) Our results suggest that the "coarse" grid (35, 110) overestimates the EIE and the "SG1" grid (50, 194) slightly underestimates it, whereas the

https://dx.doi.org/10.1021/jacs.9b11988
J. Am. Chem. Soc. 2020, 142, 1556−1563

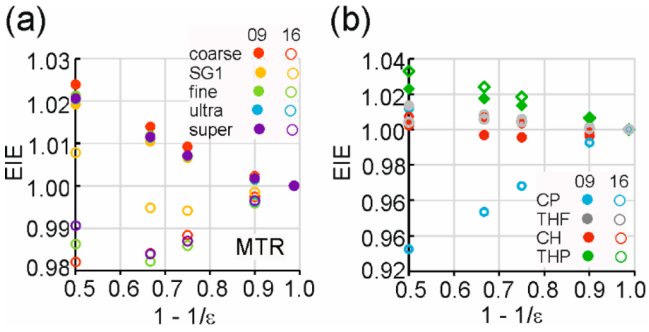

Figure 3. B3LYP/6-31+G(d)/PCM EIEs (298 K) as a function of relative permittivity for transfer from $\varepsilon = 80$ to a dielectric continuum ($2 \leq \varepsilon \leq 80$) of (a) MTR cation ($\alpha$–T EIE) for DFT integration grids of varying size and (b) of CP, THF, CH, and THP cations (α-D) with Gaussian09 or Gaussian16 PCM defaults.

"fine" grid (75, 302) gives values very close to those of the "ultrafine" (99, 590) and "superfine" (175, 974) grids, which yield essentially identical EIEs. However, using G16 defaults with the PCM method suggests a different pattern. Each grid leads to an inverse (<1) EIE for most values of ε, with some upward curvature for the very least polar media. The ultrafine and superfine grids again give virtually identical results, but these trend in the opposite direction from the G09 values. It appears that the self-consistent reaction field method employed in G16 "defaults to the symmetric form of IEFPCM (not present in G09) rather than the nonsymmetric version".[43]

It is instructive to relate IPFR values to Gibbs energies by means of $\Delta G = -RT\ln(f)$: substituting a heavier isotope into a molecule always stabilizes it ($\Delta G < 0$) since vibrational frequencies are lowered and f is always >1. Table 1 shows the magnitudes of the Gibbs energy changes for α–T substitution into MTR cation at 298 K as determined for $\varepsilon = 2$ and 80 for each of the DFT integration grids with B3LYP/6-31+G(d). The values for different grids vary by <0.1 kJ mol^{-1} and are identical for the G16 and G09 PCM defaults at $\varepsilon = 80$. However, G16 predicts $\Delta\Delta G = +0.023$ kJ mol^{-1} for transfer from "water" ($\varepsilon = 80$) to "cyclohexane" ($\varepsilon = 2$) for the superfine grid, but G09 predicts $\Delta\Delta G = -0.051$ kJ mol^{-1}, i.e., a change in the opposite direction.

Table 1. B3LYP/6-31+G(d)/PCM Negative Gibbs Energies (298 K) for α–T Substitution in MTR Cation

	G16 defaults		G09 defaults	
grid	$\varepsilon = 80$	$\varepsilon = 2$	$\varepsilon = 80$	$\varepsilon = 2$
coarse	13.005	13.050	13.005	12.946
SG1	12.935	12.916	12.935	12.888
fine	12.944	12.978	12.944	12.892
ultrafine	12.941	12.965	12.941	12.891
superfine	12.942	12.965	12.942	12.891

Figure 3b shows B3LYP/6-31+G(d) PCM/UFF α-D EIEs (298 K) for transfer of CP, THF, CH, and THP cations from $\varepsilon = 80$ to a dielectric continuum ($2 \leq \varepsilon \leq 80$), computed with ultrafine integration grids. Use of G09 defaults within G16 leads to a normal EIE for transfer from "water" to "cyclohexane" for each cation with magnitudes in the range from 1.002 (CH) to 1.023 (THP); note that the EIE for CH is inverse for $2 < \varepsilon < 80$. Use of G16 defaults also leads to normal EIEs for transfer from "water" to "cyclohexane" for THF (1.004), CH (1.007), and THP (1.033), but to a strongly inverse value (0.93) for CP. The $C_\alpha H$ "str", "ip", and "op" modes of CP are easily assignable and the variation with ε of their vibrational frequencies is shown in Figure 4. The behavior found for each mode, and—in particular—for "ip" and "op", is completely different depending which PCM implementation is used. This serves as a warning in regard to the use of implicit solvation models, with their well-known dependence on cavity shape and size, for calculations of IEs. A better approach is to consider explicitly at least those parts of the first solvation shell that make direct contact with the site of isotopic substitution.[5,20] Neglect of these specific interactions may be a reason why computed secondary EIEs and KIEs for ^{2}H or ^{3}H substitution at the anomeric C_α, are often overestimated with respect to experiment.[33]

Explicit Solvation: QM/MM Simulations in Water and Cyclohexane. For each cation (CP, THF, CH, and THP) in each solvent, consideration of all the converged structures from DFT solute relaxation within different MM solvent configurations yielded an average IPFR for α-D substitution, ratios of which gave the average K_H/K_D values presented in Table 2 for transfer from water to cyclohexane at 298 K. These EIEs show that the QM/MM treatment of explicit solvation leads to isotope effects of larger magnitude than predicted by the PCM method for implicit solvation. In all cases the lighter isotopolog prefers the looser environment provided by the nonpolar solvent. It is not possible to infer from these results how much

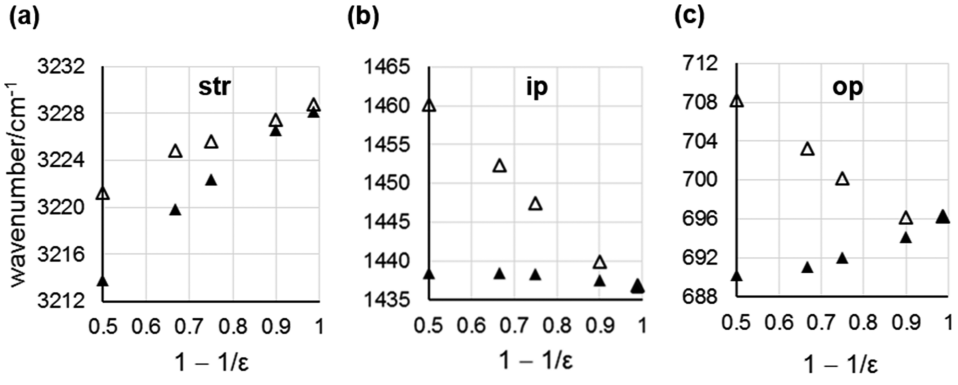

Figure 4. Variation of ultrafine B3LYP/6-31+G(d)/PCM harmonic vibrational wavenumbers for (a) $C_\alpha H$ stretching, (b) in-plane $C_\alpha H$ bending, and (c) out-of-plane $C_\alpha H$ bending of CP with relative permittivity of the dielectric continuum ($2 \leq \varepsilon \leq 80$). Solid symbols: G09 defaults; open symbols: G16 defaults.

https://dx.doi.org/10.1021/jacs.9b11988
J. Am. Chem. Soc. 2020, 142, 1556–1563

Table 2. B3LYP/6-31+G(d)/OPLS-AA Average EIEs for Transfer of Cations CP, THF, CH, and THP from Water to Cyclohexane at 298 K[a]

	CP	THF	CH	THP
full Hessian	1.047(5)	1.053(5)	1.040(6)	1.069(6)
$C_\alpha H_\alpha$ only	1.046(5)	1.053(5)	1.039(6)	1.068(6)
H_α only	1.045(5)	1.051(5)	1.039(6)	1.068(6)
n_{water}	30	42	41	47
$n_{cyclohexane}$	42	35	35	44

[a]The digit in parentheses is the standard error of the mean, i.e., (5) = ±0.005. The number of structures over which the averages are taken is denoted by *n*.

of the effect arises from the influence of the dielectric medium or from specific solvent−solute interactions, which are included in the QM/MM method but not in the continuum model. However, it is clear that the explicit treatment of solvation predicts a normal EIE for transfer of each cation from in a very polar medium (water) to a very nonpolar medium (cyclohexane): this finding is in accord with the PCM results using G09 defaults but not G16 defaults.

Cutting down the size of the Hessian (as described above) to either a single atom (H_α at the site of isotopic substitution) or a pair of atoms (H_α and C_α to which it is attached) alters the EIE values by remarkably little. The magnitudes of the IPFRs are shifted upward by about 10% and 1% for the atomic and diatomic Hessians, respectively, relative to the full Hessian, but this shift is essentially the same in each solvent. To a very good approximation the full influence of the environment upon the isotope effect is captured by the values of the Hessian elements for the site of isotopic substitution alone. The success of the atomic Hessian analysis indicates that the EIEs for transfer of a cation between different dielectric continuums are very local properties. It is unclear how general this result might be for other EIEs, but it is unlikely to hold for KIEs for which it is essential to employ a Hessian large enough to describe correctly the transition vector (reaction-coordinate vibrational mode, with its associated imaginary frequency), which may involve concerted motion of many atoms. Nonetheless, this remarkable result does suggest the possibility of performing EIE calculations for very large systems by explicit computation of the Hessian for only a single atom, although it must be understood that the quality of the QM (or QM/MM) description of that Hessian must be adequate, which may require the QM region to be much larger than the Hessian.

CONCLUDING REMARKS

We have demonstrated that EIEs (and, by implication, KIEs) may be dependent upon the polarity of the bulk medium in which a chemical process or reaction occurs. This can be thought of equivalently as "a solvent effect upon an isotope effect" or as an isotope effect upon a transfer between media of differing polarity. There are, of course, many factors that determine the magnitude and direction of isotope effects in diverse fields of study that have been well documented.[1,2,44]

However, the direct influence of the dielectric environment on isotopically sensitive vibrational frequencies, and thence upon an EIE or KIE, has not been received much attention. Reichardt and Welton's authoritative text[9] contains a section about solvent effects on infrared spectra but makes no mention of isotope effects. Undoubtedly there are good reasons why it is experimentally impractical to study the same chemical reaction in a variety of solvents of widely differing polarity; however, an advantage of computational simulation is that it is not limited by these practical constraints.

Implicit modeling of solvation by means of the PCM method clearly shows that vibrational frequencies, IPFRs and EIEs are particularly sensitive to low values of the relative permittivity of the surrounding dielectric continuum, although this seems to depend upon specific features of each molecule's cavity shape in a poorly understood way. Moreover, and unfortunately, it is evident that different implementations of nominally the same PCM method can lead to opposite trends being predicted for the same molecule. It is well-known that continuum models cannot treat specific interactions between a solute and first-solvation-shell solvent molecules. Although in principle this might be an issue for aqueous solvation of the carbenium and oxacarbenium cations considered in this work, in practice it is not: IPFRs for solutes in media with $\varepsilon > 20$ are very similar for PCM calculations with either G09 or G16 defaults. Specific solute−solvent interactions are unimportant for very nonpolar media, and a continuum treatment ought to work well for solvents such as cyclohexane; however, this does not appear to be the case. An explicit description of solvation is much more laborious, not least because it requires averaging over a representative sample of solvated configurations, but it does offer a means by which to discriminate between the contradictory predictions of an implicit treatment. Our results have decided clearly in favor of the G09 defaults in the PCM method for the evaluation of IPFRs and EIEs.

Computational modeling of the influence of the inhomogeneous effective dielectric surrounding a substrate within the protein environment of an enzymic reaction requires an explicit treatment, since an implicit method is inappropriate. A cutoff treatment with an arbitrary value of the relative permittivity of the surrounding dielectric continuum is inadequate: what value for ε should be used? This approach could yield almost any answer in view of the sensitivity of vibrational frequencies and IPFRs in the range $2 \leq \varepsilon \leq 10$, and it would render almost meaningless the attempted interpretation of calculated KIEs in terms of structural features alone of the enzymic TS. In this work we have shown that EIEs can indeed be obtained from a Hessian computed for as few atoms as the single site of isotopic substitution, but it is essential that the values of these few Hessian elements adequately reflect the full influence of the whole environment.

Variations in KIEs for families of mutant enzymes should be interpreted with great caution. The consequence of a particular amino-acid replacement may include not only a geometrical change in the structure of the TS for the enzyme−substrate complex but—in general—also a change in the electrostatic environment within which the enzymic reaction occurs.[7] Computational simulation using QM/MM methods with ensemble averaging has an important role to play in assisting the meaningful interpretation of observed isotope effects for chemical reactions both in solution and catalyzed by enzymes.

ASSOCIATED CONTENT

Supporting Information

The Supporting Information is available free of charge at https://pubs.acs.org/doi/10.1021/jacs.9b11988.

Full details of computational methods and results for PCM and QM/MM calculations of IPFRs and EIEs, including atomic Hessian analysis (PDF)

https://dx.doi.org/10.1021/jacs.9b11988
J. Am. Chem. Soc. 2020, 142, 1556−1563

AUTHOR INFORMATION

Corresponding Author

Ian H. Williams − *University of Bath, Bath, United Kingdom;* orcid.org/0000-0001-9264-0221; Email: i.h.williams@bath.ac.uk

Other Authors

Katarzyna Świderek − *Universitat Jaume I, Castellón, Spain, and University of Bath, Bath, United Kingdom;* orcid.org/0000-0002-7528-1551

Alexander J. Porter − *University of Bath, Bath, United Kingdom*

Catherine M. Upfold − *University of Bath, Bath, United Kingdom*

Complete contact information is available at: https://pubs.acs.org/10.1021/jacs.9b11988

Notes

The authors declare no competing financial interest.

ACKNOWLEDGMENTS

KŚ thanks the Esther Parkin Trust for support and the University of Bath for access to facilities during her stay as a Visiting Academic, the Ministry of Economy and Competitiveness for a Juan de la Cierva − Incorporación (ref IJCI-2016-27503) contract, and the Informatic Center of Lodz University of Technology for generous allotment of computer time on the Blueocean supercomputer. This research made use of the Balena High Performance Computing Service at the University of Bath.

REFERENCES

(1) *Isotope Effects in Chemistry and Biology*; Kohen, A., Limbach, H.-H., Eds.; Taylor and Francis: New York, 2006.

(2) *Enzyme Mechanism from Isotope Effects*; Cook, P. F., Ed.; CRC Press: Boca Raton, 1991.

(3) Rodgers, J.; Femec, D. A.; Schowen, R. L. Isotopic mapping of transition-state structural features associated with enzymic catalysis of methyl transfer. *J. Am. Chem. Soc.* **1982**, *104*, 3263−3268.

(4) Berti, P. J.; Schramm, V. L. Transition state structure of the solvolytic hydrolysis of NAD^+. *J. Am. Chem. Soc.* **1997**, *119*, 12069−12078.

(5) Wilson, P. B.; Weaver, P. J.; Greig, I. R.; Williams, I. H. Solvent effects on isotope effects: methyl cation as a model system. *J. Phys. Chem. B* **2015**, *119*, 802−809.

(6) Wilson, P. B.; Williams, I. H. Influence of equatorial CH···O interactions on secondary kinetic isotope effects for methyl transfer. *Angew. Chem., Int. Ed.* **2016**, *55*, 3192−3195.

(7) Świderek, K.; Tuñón, I.; Williams, I. H.; Moliner, V. Insights on the origin of catalysis glycine *N*-methyltransferase catalysis from computational modelling. *J. Am. Chem. Soc.* **2018**, *140*, 4327−4334.

(8) Patargias, G. N.; Harris, S. A.; Harding, J. H. A demonstration of the inhomogeneity of the local dielectric response of proteins by molecular dynamics simulations. *J. Chem. Phys.* **2010**, *132*, 235103.

(9) *Solvents and Solvent Effects in Organic Chemistry*, 4th ed.; Reichardt, C., Welton, T., Eds.; Wiley-VCH: Weinheim, Germany, 2011.

(10) Westaway, K. C. Using kinetic isotope effects to determine the structure of the transition states of S_N2 reactions. *Adv. Phys. Org. Chem.* **2006**, *41*, 217−273.

(11) Szylhabel-Godala, A.; Madhavan, S.; Rudziński, J.; O'Leary, M. H.; Paneth, P. Nitrogen and deuterium kinetic isotope effects on the Menshutkin reaction. *J. Phys. Org. Chem.* **1996**, *9*, 35−40.

(12) Owczarek, E.; Kwiatkowski, W.; Lemieszewski, M.; Mazur, A.; Rostkowski, M.; Paneth, P. Calculations of substituent and solvent effects on the kinetic isotope effects of Menshutkin reactions. *J. Org. Chem.* **2003**, *68*, 8232−8235.

(13) Yamataka, H.; Tamura, S.; Hanafusa, T.; Ando, T. Kinetic isotope effect study of the borderline solvolysis of isopropyl *β*-naphthalenesulfonate. *J. Am. Chem. Soc.* **1985**, *107*, 5429−5434.

(14) Shiner, V. J. Deuterium isotope effects in solvolytic substitution. In *Isotope Effects in Chemical Reactions*; Collins, C. J., Bowman, N. S., Eds.; Van Nostrand Reinhold: New York, 1970.

(15) Bentley, T. W. Secondary *α*-deuterium kinetic isotope effects: assumptions simplifying interpretations of mechanisms of solvolyses of secondary alkyl sulfonates. *J. Org. Chem.* **2004**, *69*, 1756−1759.

(16) Shiner, V. J.; Buddenbaum, W. E.; Murr, B. L.; Lamaty, G. Effects of deuterium substitution on the rates of organic reactions. XI. *α*- and *β*-Deuterium effects on the solvolysis rates of a series of substituted 1-phenylethyl halides. *J. Am. Chem. Soc.* **1968**, *90*, 418−426.

(17) Keller, J. H.; Yankwich, P. E. Medium effects on heavy-atom kinetic isotope-effects 0.1. Cell model without internal-external coordinate interaction. *J. Am. Chem. Soc.* **1973**, *95*, 4811−4815.

(18) Keller, J. H.; Yankwich, P. E. Medium effects on heavy-atom kinetic isotope-effects 0.2. Cell model with external-external and certain external-internal coordinate interactions. *J. Am. Chem. Soc.* **1973**, *95*, 7968−7972.

(19) Keller, J. H.; Yankwich, P. E. Medium effects on heavy-atom kinetic isotope-effects 0.3. Structured medium model applied to complex-formation via mass point attachment and coupling. *J. Am. Chem. Soc.* **1974**, *96*, 2303−2314.

(20) Wilson, P. B.; Williams, I. H. In *Simulating Enzyme Reactivity: Computational Methods in Enzyme Catalysis*; Tuñón, I., Moliner, V., Eds.; Royal Society of Chemistry: Cambridge, 2017.

(21) Frisch, M. J. et al. *Gaussian 09*, Revision A.02; Gaussian, Inc.: Wallingford CT, 2009.

(22) Wilson, P. B.; Williams, I. H. Computational modelling of a caged methyl cation: structure, energetics and vibrational analysis. *J. Phys. Chem. A* **2018**, *122*, 1432−1438.

(23) Glancy, J. H.; Lee, D. M.; Read, E. O.; Williams, I. H. Computational simulation of mechanism and isotope effects on acetal heterolysis as a model for glycoside hydrolysis. *Pure Appl. Chem.* **2019**, DOI: 10.1515/pac-2019-0221.

(24) Wilson, P. B.; Williams, I. H. Critical evaluation of anharmonic corrections to the equilibrium isotope effect for methyl cation transfer from vacuum to dielectric continuum. *Mol. Phys.* **2015**, *113*, 1704−1711.

(25) Frisch, M. J. et al. *Gaussian 16*, Revision A.03; Gaussian, Inc.: Wallingford CT, 2016.

(26) Williams, I. H.; Wilson, P. B. SULISO: The Bath suite of vibrational characterization and isotope effect calculation software. *SoftwareX* **2017**, *6*, 1−6.

(27) Williams, I. H. On the representation of force fields for chemically reacting systems. *Chem. Phys. Lett.* **1982**, *88*, 462−466.

(28) Williams, I. H. Force-constant computations in Cartesian coordinates. Elimination of translational and rotational contributions. *J. Mol. Struct.: THEOCHEM* **1983**, *94*, 275−284.

(29) Martinez, L.; Andrade, R.; Birgin, E. G.; Martinez, J. M. Packmol: A package for building initial configurations for molecular dynamics simulations. *J. Comput. Chem.* **2009**, *30*, 2157−2164.

(30) Field, M. J. *A Practical Introduction to the Simulation of Molecular Systems*; Cambridge University Press: Cambridge, U.K., 1999.

(31) Field, M. J.; Albe, M.; Bret, C.; Proust-de Martin, F.; Thomas, A. The Dynamo library for molecular simulations using hybrid quantum mechanical and molecular mechanical potentials. *J. Comput. Chem.* **2000**, *21*, 1088−1100.

(32) Ruiz-Pernía, J. J.; Williams, I. H. Ensemble-averaged QM/MM kinetic isotope effects for the S_N2 reaction of cyanide anion with chloroethane in DMSO solution. *Chem. - Eur. J.* **2012**, *18*, 9405−9414.

(33) Singh, V.; Schramm, V. L. Transition-state analysis of *S. pneumoniae* 5′-methylthioadenosine nucleosidase. *J. Am. Chem. Soc.* **2007**, *129*, 2783−2795.
(34) Wilson, E. B.; Decius, J. C.; Cross, P. C. *Molecular Vibrations*; McGraw-Hill: New York, 1955.
(35) Wolfsberg, M. Comments on selected topics in isotope theoretical chemistry. In *Isotope Effects in Chemistry and Biology*; Kohen, A., Limbach, H.-H., Eds.; Taylor and Francis: New York, 2006.
(36) Ahmad, I. A.; Birkby, S. L.; Bullen, C. A.; Groves, P. D.; Lankau, T.; Lee, W. H.; Maskill, H.; Miatt, P. C.; Menneer, I. D.; Shaw, K. Hydrolysis of 2-(*p*-nitrophenoxy)tetrahydropyran: solvent and a-deuterium secondary kinetic isotope effects and relationships with the solvolysis of simple secondary alkyl arenesulfonates and the enzyme-catalyzed hydrolysis of glycosides. *J. Phys. Org. Chem.* **2004**, *17*, 560−566.
(37) Wolfsberg, M.; Stern, M. J. Validity of some approximation procedures used in the theoretical calculation of isotope effects. *Pure Appl. Chem.* **1964**, *8*, 225−242.
(38) Stern, M. J.; Wolfsberg, M. Simplified procedure for the theoretical calculation of isotope effects involving large molecules. *J. Chem. Phys.* **1966**, *45*, 4105−4124.
(39) Melander, L.; Saunders, W. H. *Reaction Rates of Isotopic Molecules*; Wiley: New York, 1980.
(40) Born, M. Volumen und hydrationswarme der ionen. *Eur. Phys. J. A* **1920**, *1*, 45−48.
(41) Onsager, L. Electric moments of molecules in solution. *J. Am. Chem. Soc.* **1936**, *58*, 1486−1493.
(42) Bootsma, A. N.; Wheeler, S. Popular integration grids can result in large errors in DFT-computed free energies. *ChemRxiv*. DOI: 10.26434/chemrxiv.8864204.v1.
(43) https://gaussian.com/relnotes/ (accessed October 10, 2019).
(44) *Isotope Effects in the Chemical, Geological and Bio Sciences*; Wolfsberg, M., Van Hook, A., Paneth, P., Eds.; Springer: London, 2010.

https://dx.doi.org/10.1021/jacs.9b11988
J. Am. Chem. Soc. 2020, 142, 1556−1563